Solvent Activity in Electrolyte Solutions from Molecular Simulation of the Osmotic Pressure

Maximilian Kohns, Steffen Reiser, Martin Horsch[1], Hans Hasse

University of Kaiserslautern, Laboratory of Engineering Thermodynamics, Erwin-Schrödinger Str. 44, D-67663 Kaiserslautern, Germany

Abstract

A novel method for determining the activity of the solvent in electrolyte solutions by molecular dynamics simulations is presented. The electrolyte solution is simulated in contact with the pure solvent. Between the two phases, there is a virtual membrane, which is permeable only for the solvent. In the simulation, this is realized by an external field which acts on the solutes only, and confines the solutes to a part of the simulation volume. The osmotic pressure, i.e. the pressure difference of both phases, is obtained with high accuray from the force on the membrane, so that reliable data on the solvent activity can be determined. The acronym of the new method is therefore OPAS (osmotic pressure for activity of solvents). The OPAS method is validated using test cases of varying complexity and compared to

[1]Corresponding author; martin.horsch@mv.uni-kl.de; phone: +49-631 / 205-3227; fax: +49-631 / 205-3835.

different other methods from the literature using aqueous sodium chloride solutions as an example.

Keywords: Electrolyte solution, Osmotic pressure, Solvent activity, Molecular dynamics

---

1. Introduction

Electrolyte solutions are important in many industrial and natural processes. Even though the most important solvent is water, also organic electrolyte solutions are highly interesting, e.g. in energy storage technology. The thermodynamic behavior of electrolyte solutions is dominated by the Coulombic interactions between ions and solvent molecules and related solvation effects. Due to this complex behavior, phenomenological models for describing electrolyte solutions often employ a large number of adjustable parameters to correlate experimental data [1–4]. Another shortcoming is that the model parameters are not transferable when different solvents are used. Molecular simulations provide an opportunity to gain insight into the inner workings of electrolyte solutions on the molecular level. In contrast to phenomenological models, molecular simulation usually takes into account only binary interactions between species. Additionally, properties of mixtures can be predicted if accurate molecular models for all components are available.

One of the most important properties of an electrolyte solution is the activity of the solvent. It is directly related to phenomena such as vapor pressure lowering and freezing point depression, and it is connected to the activity coefficient of the salt, which controls the solubility limit of the salt. However, the reliable determination of the solvent activity and related properties of electrolyte solutions by molecular simulations is challenging and subject to recent research.

In a series of papers, Smith and co-workers [5–9] developed the OEMC method for the computation of solubility limits in electrolyte solutions. The method employs a semi-grand ensemble to compute the salt molality m at a given chemical potential of the salt $\mu_{\pm}$ in a Monte Carlo (MC) simulation. In a recent paper, Mester and Panagiotopoulos [10] conducted molecular dynamics (MD) simulations in the isothermal-isobaric (NpT) ensemble to determine the chemical potential of the salt $\mu_{\pm}$ at a given salt molality m by performing fractional insertion of ion pairs. Using the Gibbs-Duhem equation, the solvent activity a_{solv} can be derived from the results of either method. Both works have in common that advanced sampling methods were used to improve the statistics, as particle insertion moves for ions are very unlikely to be accepted [6].

In previous work of our group [11, 12], a set of molecular models for alkali and halide ions in conjunction with the SPC/E [13] water model has been developed. Simulation results using these models have shown good agreement with available experimental data for various properties such as liquid solution densities, radial distribution functions, diffusion coefficients and electric conductivities [14]. Furthermore, the model parameters are transferable so that methanolic and ethanolic electrolyte solutions can also be described [15, 16]. The most important property that has not yet been investigated with these models is the solvent activity.

In the present work, a novel method is introduced for molecular dynamics simulation of the osmotic pressures for determining the activity of solvents (OPAS). The OPAS method circumvents the problems regarding particle insertion. OPAS simulations exploit the relationship between the solvent activity and the osmotic pressure by performing simulations of coexisting phases in osmotic equilibrium, i.e. a pure solvent phase and an electrolyte solution phase in direct contact. The phases are separated by a semipermeable membrane, which is permeable for the solvent but not for the solutes (here: the ions). The idea of such direct coexistence simulations goes back to a series of papers by Murad and co-workers [17–20], who used Lennard-

Jones (LJ) particles to which they applied a position constraint to simulate a semipermeable membrane. The present OPAS simulation method follows an approach which is similar to that of Luo and Roux [21], who use a virtual semipermeable membrane. The OPAS method adopts the general simulation scenario of Luo and Roux and extends their work regarding the simulation methodology and the evaluation of the results.

In Section 2, the OPAS method is presented. The thermodynamic consistency of this new method is described in Sections 3 and 4. Section 5 summarizes the main findings and mentions further applications for the OPAS method.

2. OPAS Simulation Method

The OPAS molecular dynamics simulation method directly computes the osmotic equilibrium in mixtures with virtual semipermeable membranes. The method is mainly intended for studying electrolyte solutions, but can in principle be used for any kind of binary mixture. An extension to more than one solute is straightforward, an extension to mixed solvents is possible.

To simulate the osmotic equilibrium, two planar, semipermeable membranes M1 and M2 are introduced in the cubic simulation box. They are located at

the positions $z_{\mathrm{M1}} = 0.25\ L$ and $z_{\mathrm{M2}} = 0.75\ L$, where L is the box length, and therefore lie parallel to the x, y-plane. The membranes divide the simulation volume into two compartments. The outer compartment ($0 \leq z/L < 0.25$ and $0.75 < z/L \leq 1$) contains only solvent molecules, while the inner compartment ($0.25 \leq z/L \leq 0.75$) contains both solvent and solute molecules. The conventional periodic boundary conditions are used. A snapshot of this simulation setup is shown in Figure 1.

[Figure 1 about here.]

If a solute molecule i leaves the inner compartment at either M1 or M2, a force

$$\text{for } z_i < z_{\mathrm{M1}}: \quad F_i = c(z_{\mathrm{M1}} - z_i) \tag{1}$$

$$\text{for } z_i > z_{\mathrm{M2}}: \quad F_i = c(z_{\mathrm{M2}} - z_i) \tag{2}$$

is exerted on it in the z direction, where z_i is the z-component of the center of mass position of ion i. The value of the membrane force constant $c = 4.184 \cdot 10^{24}\ \mathrm{J/m^2}$ was taken from Luo and Roux [21]. The osmotic pressure is the pressure difference of both compartments and is obtained from the

membrane force as

$$\Pi = p_{\mathrm{in}} - p_{\mathrm{out}} = \frac{F_{\mathrm{tot}}}{A_{\mathrm{tot}}} = \frac{\sum_i |F_i|}{A_{\mathrm{M1}} + A_{\mathrm{M2}}}, \tag{3}$$

where F_{tot} is the total net force on both membranes and A_{tot} is their total area.

It is desirable to simulate the osmotic equilibrium at a specified pressure $p_{\mathrm{out}} = p_{\mathrm{set}}$ in the outer compartment, i.e. in the pure solvent phase (typically $p_{\mathrm{set}} = 1$ bar). However, a direct run in the canonical (NVT) ensemble is not convenient as the resulting pressure p_{out} is hard to guess. Therefore, an OPAS simulation consists of a two-step procedure.

First, a pseudo-isothermal-isobaric (NpT) ensemble simulation is carried out for determining the box volume $\langle V \rangle$ of the system in osmotic equlibrium while $p_{\mathrm{out}} = p_{\mathrm{set}}$. To avoid the necessity of a specially designed barostat for that purpose, the entire system is coupled to a barostat that yields the effective pressure

$$p_{\mathrm{eff}} = (p_{\mathrm{out}} V_{\mathrm{out}} + p_{\mathrm{in}} V_{\mathrm{in}})/(V_{\mathrm{out}} + V_{\mathrm{in}}). \tag{4}$$

The effective pressure p_{eff} corresponds to an average over the virial of the entire system. The pressure in the outer compartment p_{out} is fixed to p_{set} and p_{in} can be estimated on the fly from $p_{\mathrm{in}} = p_{\mathrm{out}} + \Pi$, where Π is obtained

by Eq. (3). As a result, the desired pressure p_{set} is obtained in the outer compartment and an estimate of the box volume $\langle V \rangle$ is obtained. Furthermore, this pseudo-NpT run serves as a pre-equilibration of the system. Note that for the specific choice of compartment volumes $V_{\mathrm{out}} = V_{\mathrm{in}}$ in the present work, Eq. (4) simplifies to

$$p_{\mathrm{eff}} = p_{\mathrm{out}} + \frac{\Pi}{2}. \tag{5}$$

The volume $\langle V \rangle$ is then used in a canonical (NVT) ensemble simulation, which yields the osmotic pressure $\langle \Pi \rangle = \langle F_{\mathrm{tot}} \rangle / A_{\mathrm{tot}}$ of the system. The osmotic pressure is directly related to the solvent activity via

$$\ln(a_{solv}) = -\frac{\Pi}{\rho_{solv} RT}, \tag{6}$$

when an incompressible solvent is assumed, R is the universal gas constant, and ρ_{solv} is the density of the pure liquid solvent at the temperature T. This property is available from separate molecular simulations. A derivation of Eq. (6) is given in Appendix A.

During the simulation, the electrolyte molality in the inner compartment fluctuates as water molecules are free to move. Therefore, the composition of the inner compartment is a simulation output, and a density profile is recorded for all components in the NVT run. In order to exclude artifacts

present in the vicinity of the membranes, the density of the solvent should only be averaged over a part of the inner compartment. In this work, this region is chosen to be $0.4 \leq z/L \leq 0.6$, which from here on is referred to as the inner sampling volume, but another suitable choice might as well be made. However, this specific choice of the inner sampling volume has proven to be reliable in the present work. The averaged density of the solvent $\overline{\rho}_{solv}$ in the inner sampling volume is then used to compute the mole fraction of the solvent in the inner compartment via

$$x_{solv} = \overline{\rho}_{solv} \left(\overline{\rho}_{solv} + \sum_{i=1}^{N_{\text{solutes}}} \rho_i \right)^{-1} . \tag{7}$$

Note that the exact densities of the solutes ρ_i are known as the number of solute molecules is an input of the simulation and the solute molecules are always in the inner compartment.

When considering electrolyte solutions, activity coefficients and related quantities are usually expressed in terms of the salt molality m instead of mole fractions. The conversion from the ion-based mole fraction of the solvent x_{solv}, obtained by Eq. (7), to the salt molality and a corresponding estimation of the statistical uncertainty of this quantity is given in Appendix B.

Altogether, the OPAS method has the following set of simulation parameters:

- the membrane positions z_{M1} and z_{M2}, or, respectively, the compartment

volume ratio $V_{\mathrm{in}}/V_{\mathrm{out}}$

- the number of particles N
- the choice of the inner sampling volume for the evaluation of the density profile
- the membrane force constant c

Obviously, a symmetric arrangement of the membranes seems convenient, as it leads to a simple modification of a standard barostat (see Eq. (5)). It might be advantageous to use a box elongated in z-direction, however, this would automatically lead to a larger number of particles. In the present work, it was found that $N = 4000$ is sufficient to obtain smooth density profiles in a broad inner sampling volume of $0.4 \leq z/L \leq 0.6$ (cf. Section 4). Therefore, a different arrangement is unnecessary. The impact of the membrane force constant c was studied in a number of preliminary runs and was found to be small. Furthermore, the good agreement of OPAS results with results of other methods from the literature [9, 10] shows that the choice of c adopted from Luo and Roux [21] is appropriate (cf. Section 4).

All simulations of this study were carried out with an extended version of the molecular simulation program $ms2$ [22]. More simulation details are given in

Appendix C.

3. Validation of the Simulation Method

3.1. Validation approach

Test cases of varying complexity were set up in order to check the thermodynamic consistency of simulation results obtained by OPAS simulations. The OPAS simulations must satisfy three conditions:

- The system size must be sufficient, so that the partial density of the solvent in the inner sampling volume is not influenced by the membranes.
- The osmotic pressure Π obatined from sampling the membrane force must be equal to the pressure difference $\Delta p = p_{\text{in}} - p_{\text{out}}$ computed from the pressure profile.
- The chemical potential of the solvent must be constant over the coordinate z normal to the membranes.

The first condition can be checked by inspection of the density profile. For the second condition, a pressure profile $p(z)$ was recorded for the test cases. As for the evaluation of the density profiles, sampling volumes have to be

defined. In this work, the inner sampling volume for the pressure was chosen to be the same as that for the densities ($0.4 \leq z/L \leq 0.6$), and accordingly, for the outer sampling volume the choice ($0 \leq z/L < 0.1$ and $0.9 < z/L \leq 1$) was made. By averaging over both sampling volumes, an estimate of the pressure difference $\Delta p = \overline{p}_{\mathrm{in}} - \overline{p}_{\mathrm{out}}$ is obtained. For the third condition, a profile of the reduced residual chemical potential of the solvent $\tilde{\mu}_{solv}(z)$ was recorded. It is defined by Vrabec and Hasse [23] as

$$\tilde{\mu}_{solv} = \frac{\mu_{solv} - \mu_{solv}^{\mathrm{id}}(T)}{kT}, \tag{8}$$

where k is Boltzmann's constant. If all three conditions are fulfilled, one can conclude that the OPAS method is applicable for the respective test case.

3.2. Molecular models

The test cases for the OPAS method consist of different molecular model classes. Depending on the test case, the total potential energy contains Lennard-Jones (LJ) contributions only, or charge-charge or quadrupole-quad-

rupole interactions also, and thus writes as

$$
\begin{aligned}
U &= U_{\mathrm{LJ}} + U_{\mathrm{CC}} + U_{\mathrm{QQ}} \\
&= \sum_{i=1}^{N-1} \sum_{j=i+1}^{N} \left\{ \sum_{a=1}^{n_i^{\mathrm{LJ}}} \sum_{b=1}^{n_j^{\mathrm{LJ}}} 4\epsilon_{ijab} \left[\left(\frac{\sigma_{ijab}}{r_{ijab}} \right)^{12} - \left(\frac{\sigma_{ijab}}{r_{ijab}} \right)^{6} \right] \right. \\
&\quad \left. + \sum_{c=1}^{n_i^e} \sum_{d=1}^{n_j^e} \frac{1}{4\pi\epsilon_0} \left[\frac{q_{ic} q_{jd}}{r_{ijcd}} + \frac{Q_{ic} Q_{jd}}{r_{ijcd}^5} \cdot f(\omega_i, \omega_j) \right] \right\},
\end{aligned} \tag{9}
$$

where ϵ_{ijab} and σ_{ijab} are the Lennard-Jones energy and size parameters, r_{ijab} and r_{ijcd} are site-site distances, q_{ic}, q_{jd}, Q_{ic} and Q_{jd} are the magnitude of the electrostatic interactions, i.e. the point charges and quadrupole moments. Therein, $f(\omega_i, \omega_j)$ is a dimensionless angle-dependent expression in terms of the orientation (ω_i,ω_j) of the point quadrupoles [24].

The modified Lorentz-Berthelot combining rules are used [25, 26] for the interaction between unlike Lennard-Jones sites

$$\sigma_{ij} = \frac{\sigma_{ii} + \sigma_{jj}}{2}, \tag{10}$$

$$\epsilon_{ij} = \xi_{ij} \sqrt{\epsilon_{ii} \epsilon_{jj}}. \tag{11}$$

The binary interaction parameter ξ_{ij} is set to 1 for all combinations except for the test case 'argon + O_2 mixture', where the value $\xi_{\mathrm{Ar,O2}} = 0.988$ adjusted by Vrabec et al. [27] is used. Table 1 gives an overview of the test cases.

[Table 1 about here.]

3.3. Binary LJ mixture I

The first test case for the OPAS method is a liquid binary LJ mixture. The solvent A and the solute B are equal LJ species, i.e. $\sigma_{\mathrm{B}}/\sigma_{\mathrm{A}} = 1.0$ and $\epsilon_{\mathrm{B}}/\epsilon_{\mathrm{A}} = 1.0$. The only difference is that the solvent molecules of component A are free to pass the membrane, while the solute molecules of component B are not. For this test case, only the NVT run has been performed to independently validate this step of an OPAS simulation. The state point used for this test case is $T = 1.2\ \epsilon_{\mathrm{A}}/k$ and $\rho = 0.6\ \sigma_{\mathrm{A}}^{-3}$. The system consists of $N_{\mathrm{A}} = 3600$ solvent molecules and $N_{\mathrm{B}} = 400$ solute molecules. Therefore, initially, the partial densities in the outer compartment are $\rho_{\mathrm{A,out}}^{\mathrm{init}} = 0.6\ \sigma_{\mathrm{A}}^{-3}$ and $\rho_{\mathrm{B,out}}^{\mathrm{init}} = 0.0\ \sigma_{\mathrm{A}}^{-3}$ as well as $\rho_{\mathrm{A,in}}^{\mathrm{init}} = 0.48\ \sigma_{\mathrm{A}}^{-3}$ and $\rho_{\mathrm{B,out}}^{\mathrm{init}} = 0.12\ \sigma_{\mathrm{A}}^{-3}$ in the inner compartment. The cut-off radius is $r_{\mathrm{cut}} = 6.5\ \sigma_{\mathrm{A}}$.

3.4. Binary LJ mixture II

The second test case for the OPAS method is similar to the first one. Both solvent A and solute B are LJ species sharing the same size parameter, but with different energy parameters, i.e. $\sigma_{\mathrm{B}}/\sigma_{\mathrm{A}} = 1.0$ and $\epsilon_{\mathrm{B}}/\epsilon_{\mathrm{A}} = 0.66$. As for the first test case, only the NVT run has been performed. The state point used is $T = 1.0\ \epsilon_{\mathrm{A}}/k$ and $\rho = 0.7\ \sigma_{\mathrm{A}}^{-3}$. The system consists of $N_{\mathrm{A}} = 3600$ solvent molecules and $N_{\mathrm{B}} = 400$ solute molecules. The cut-off radius is

$r_{\mathrm{cut}} = 6.5\ \sigma_{\mathrm{A}}$.

3.5. Argon + O_2 mixture

The third test case for the OPAS method is a liquid mixture of the solvent Argon and the solute O_2. The molecular models developed by Vrabec et al. [28] were used for both species. The binary interaction parameter $\xi_{\mathrm{Ar,O2}} = 0.988$ is taken from Vrabec et al. [27]. Again, only the NVT run was performed. The state point used is $T = 140$ K and $\rho = 26$ mol l^{-1}. The system consists of $N_{\mathrm{Ar}} = 3600$ solvent and $N_{\mathrm{O2}} = 400$ solute molecules. The cut-off radius is $r_{\mathrm{cut}} = 22.75$ Å.

3.6. Aqueous NaCl solution I

The last test case for the OPAS method is an aqueous NaCl solution, where the Na^+ and Cl^- ion models of Joung and Cheatham [29] (JC) are used together with the SPC/E [13] water model. The full OPAS method was run at the state point $T = 298.15$ K and $p_{\mathrm{out}} = 1$ bar. The system consists of $N_{\mathrm{W}} = 3920$ water molecules and $N_{\mathrm{Na^+}} = N_{\mathrm{Cl^-}} = 40$ ions, respectively. The cut-off radius is $r_{\mathrm{cut}} = 15$ Å. Note that for this simulation only the density and pressure profiles were recorded, as the profile of the chemical potential of water in an aqueous electrolyte solution cannot be obtained with standard

test particle insertion methods [6].

3.7. Aqueous NaCl solution II

The OPAS method was also used to simulate osmotic pressures for aqueous solutions at different molalities of NaCl, using the SPC/E + JC model combination and a cut-off radius of $r_{\mathrm{cut}} = 15$ Å. The state point $T = 298.15$ K and $p_{\mathrm{out}} = 1$ bar was used. This system has been investigated recently by Mester and Panagiotopoulos [10] and by Moučka et al. [9], thus allowing for a comparison of results obtained with different methods. The density $\rho_{\mathrm{SPC/E}} = 55.27$ mol l^{-1} of pure SPC/E water at $T = 298.15$ K and $p = 1$ bar is taken from Guevara-Carrion et al. [30].

4. Results and Discussion

4.1. Binary LJ mixture I

Figure 2 shows the simulation results for the binary LJ mixture.

[Figure 2 about here.]

The density profile shows a constant partial density of the solvent in the inner sampling volume. Due to the osmotic equilibrium, the pressure in the inner compartment is higher than in the outer compartment. The resulting

pressure difference $\Delta p = \overline{p}_{\text{in}} - \overline{p}_{\text{out}}$ is in agreement with the osmotic pressure Π derived from the membrane force, as can be seen in Table 1. The uncertainties for the pressure difference result from a block average of the individual pressures $p(z)$ and therefore underestimate the uncertainty slightly. Therefore, the values for Π and Δp show a slight difference, but this can be attributed to the general inaccuracy of computing the pressure profile. In contrast, the advantage of the computation via the membrane force is that it is computationally much cheaper and yield results with smaller statistical uncertainties. The statistical uncertainty using the sampling of the membrane force is about three times lower than using the pressure profile. In contrast to the density and pressure profiles, the profile of the chemical potential of the solvent remains constant over the membranes. Therefore, all three conditions for thermodynamic constistency are fulfilled for this test case.

4.2. Binary LJ mixture II

Figure 3 shows the simulation results for the test case 'unlike LJ mixture'.

[Figure 3 about here.]

As for the first test case, the density profile shows a constant partial density of the solvent in the inner sampling volume. Furthermore, the pressure difference Δp obtained from the pressure profile is in good agreement with the osmotic pressure Π derived from the membrane force, cf. Table 1. Again, the sampling of the membrane force yields three times lower statistical uncertainties for the osmotic pressure than the pressure profile. The profile of the chemical potential of the solvent remains constant over the membranes. Therefore, all three conditions for thermodynamic constistency are fulfilled for this test case as well.

4.3. Argon + O_2 mixture

Figure 4 shows the simulation results for the test case 'argon + O_2 mixture'.

[Figure 4 about here.]

All three profiles show the same behavior as for the test cases with LJ particles. A constant partial density of the solvent Argon is reached in the inner sampling volume. The osmotic pressures derived from the two independent methods are in good agreement (cf. Table 1), and the chemical potential of the solvent Argon remains constant over the box length. Therefore, all

three conditions for thermodynamic constistency are fulfilled. These results confirm that the method is valid not only for simple LJ systems, but also for models of real fluids with electrostatic interactions.

4.4. Aqueous NaCl solution I

Figure 5 shows the simulation results for the test case 'aqueous NaCl solution'.

[Figure 5 about here.]

The partial density of the solvent water is constant in the inner sampling volume. The same holds true for the partial densities of the two ions Na^+ and Cl^-, which coincide due to the electroneutrality condition. From the pressure profile in Figure 5 and from Table 1 it can be clearly seen that the computation of the osmotic pressure via the membrane force is more accurate than the evaluation of the pressure difference, as the former method leads to much smaller statistical uncertainties. Therefore, the two conditions for thermodynamic constistency that could be tested for electrolyte solutions are fulfilled for the test case 'aqueous NaCl solution'.

4.5. Aqueous NaCl solution II

Figure 6 shows the simulation results for aqueous NaCl solutions at varying salt concentrations with the SPC/E + JC model combination. The numerical simulation results are given in Table 2.

[Figure 6 about here.]

[Table 2 about here.]

Figure 6 also contains the results of Mester and Panagiotopoulos [10] and of Moučka et al. [9], who used the same molecular models, but different simulation methods. First, it can be deduced that the SPC/E + JC model combination overestimates the osmotic pressures in aqueous NaCl solutions at all salt molalities, and the deviations are more pronounced for high molalities. Consequently, the water activity is underestimated. Furthermore, the results of all three molecular simulation methods are in very good agreement, which serves as a further validation of the present OPAS simulation method.

5. Conclusions

A new molecular simulation method for the computation of solvent activities in mixtures, called OPAS simulation, was presented. The advantage of

the method lies in its simplicity, compared to methods used in other studies in the literature [5–10]. Although the OPAS method is mainly intended for studying electrolyte solutions, it was shown that it is also applicable to any kind of mixture.

The thermodynamic consistency of the method was shown using test cases of varying complexity. The simulation results suggest that the method can be applied to any kind of mixture, and it is employed here for studying electrolyte solutions. The statistical uncertainties in the target properties salt molality m, osmotic pressure Π and natural logarithm of the solvent activity $\ln(a_{solv})$ were found to be small, proving that the present simulations are highly accurate. Additionally, the simulation results agree well with results obtained with other molecular simulation methods [9, 10], which once again supports the validity of the OPAS simulation method.

By OPAS simulation, studies of various phenomena such as vapor pressure lowering or freezing point depression can be performed. Additionally, an extension of the method to compute the activity coefficient of the salt is possible, allowing for the computation of salt solubilities (if the chemical potential of the pure solid salt is known). In this way, OPAS simulations will contribute to a more profound modeling of electrolyte solutions.

Acknowledgement

The authors gratefully acknowledge financial support within the Reinhart Koselleck Program (HA1993/15-1) of the German Research Foundation (DFG). The present work was conducted under the auspices of the Boltzmann-Zuse Society of Computational Molecular Engineering (BZS) and the simulations were carried out on the Regional University Computing Center Kaiserslautern (RHRK) under the grant TUKL-MSWS as well as the High Performance Computing Center Stuttgart (HLRS) under the grant MMHBF. The authors would like to thank Stephan Deublein and Rajat Srivastava for fruitful discussions as well as Colin Glass and Jadran Vrabec for their contributions to developing the $ms2$ program.

Appendix A. Derivation of the Solvent Activity

Let $'$ denote the pure solvent phase and $''$ denote the solution phase in osmotic equilibrium at a constant temperature T. Equality of the chemical

potential of the solvent in both phases yields

$$\mu'_{solv} = \mu''_{solv} \tag{A.1}$$

$$\mu_{solv}^{\text{pure liq}}(T, p') + RT \ln a'_{solv}(T, p', \underline{x}') = \mu_{solv}^{\text{pure liq}}(T, p'') + RT \ln a''_{solv}(T, p'', \underline{x}''), \tag{A.2}$$

where $\underline{x}$ denotes the vector of mole fractions. Since $'$ is the pure solvent phase, $a'_{solv}(T, p', \underline{x}') = 1$ and thus

$$\mu_{solv}^{\text{pure liq}}(T, p'') - \mu_{solv}^{\text{pure liq}}(T, p') = -RT \ln a''_{solv}(T, p'', \underline{x}''). \tag{A.3}$$

The difference in chemical potentials can be expressed as

$$\int_{'}^{''} v_{solv}^{\text{pure liq}} \, dp = -RT \ln a''_{solv}(T, p'', \underline{x}''). \tag{A.4}$$

where $v_{solv}^{\text{pure liq}}$ is the molar volume of the solvent. Assuming and incompressible solvent, one obtains

$$v_{solv}^{\text{pure liq}}(p'' - p') = -RT \ln a''_{solv}(T, p'', \underline{x}''). \tag{A.5}$$

The pressure difference $(p'' - p')$ is the osmotic pressure Π and therefore

$$\ln a''_{solv}(T, p'', \underline{x}'') = -\frac{\Pi v_{solv}^{\text{pure liq}}}{RT}. \tag{A.6}$$

Appendix B. Conversion of concentration units

Application of Eq. (7) of the main text yields the ion-based mole fraction of the solvent, so that in case of a 1-1 electrolyte

$$x_{solv} + 2x_{ion} = 1. \tag{B.1}$$

In order to obtain the molality of the salt, the ion-based mole fraction of the solvent has to be converted to the salt-based mole fraction of the solvent

$$\tilde{x}_{solv} = 1 - \frac{x_{ion}}{1 - x_{ion}} \tag{B.2}$$

The mole fraction of the solvent can then be converted to the salt molality

$$m = \frac{\tilde{x}_{salt}}{\tilde{x}_{solv} M_{solv}} = \frac{1 - \tilde{x}_{solv}}{\tilde{x}_{solv} M_{solv}}, \tag{B.3}$$

where M_{solv} is the molecular mass of the solvent in kg mol^{-1}.

During the simulation, the statistical uncertainty of the average partial density of the solvent $\overline{\rho}_{solv}$ is monitored. It is assumed to be three times the standard deviation obtained with the block average method by Flyvbjerg and Petersen [31]. The uncertainty of the salt molality is derived by applying error propagation through all conversion steps in Eqs. (7) and (B.1) to (B.3).

Appendix C. Molecular simulation details

All simulations of this study were carried out with an extended version of the simulation program $ms2$ [22]. In $ms2$, thermophysical properties can be determined for rigid molecular models using Monte Carlo (MC) or molecular dynamics (MD) simulation techniques. For all simulations, the LJ interaction partners are determined for every time step and MC loop, respectively. Interaction energies between molecules and/or ions are determined explicitly for distances smaller than the cut-off radius r_{cut}. The thermostat incorporated in $ms2$ is velocity scaling. The pressure is kept constant using Andersens barostat in MD, and random volume changes evaluated according to Metropolis acceptance criterion in MC, respectively. The simulation uncertainties are estimated with the block average method by Flyvbjerg and Petersen [31].

The total number of particles was 4000 throughout. In all MD simulations, Newtons equations of motion were solved with a gear predictor-corrector scheme of fifth order. The long-range interactions were considered by Ewald summation [32]. The calculation of the pressure profiles is based on the method proposed by Kirkwood and Buff [33].

For the simulations of electrolyte solutions, at first simulations in a modified isothermal-isobaric (NpT) ensemble were carried out (details see main

text). A physically reasonable configuration was obtained after equilibrating for 2,000,000 time steps, followed by a production run of 10,000,000 time steps. The resulting box volume V was then used for a run in the canonical (NVT) ensemble, in which equilibration an production took 3,000,000 and 10,000,000 time steps, respectively. The time step was $\Delta t = 1.2$ fs.

For the simulations of the test cases (binary LJ mixture, unlike LJ mixture, argon + O_2 mixture), simulations were directly carried out in the canonical (NVT) ensemble. The number of time steps was the same as for the electrolyte solution, and the reduced time step was $\Delta t^* = 0.0005$. Widom's test particle insertion [34] was used to calculate the chemical potential of the solvent, and 5400 test particles were inserted at every production time step.

[1] K.S. Pitzer. *J. Phys. Chem.*, 77 (2):268–277, 1973.

[2] K.S. Pitzer and G. Mayorga. *J. Phys. Chem.*, 77 (19):2300–2308, 1973.

[3] K.S. Pitzer and G. Mayorga. *J. Solution Chem.*, 3 (7):539–546, 1974.

[4] K.S. Pitzer and J.J. Kim. *J. Am. Chem. Soc.*, 96 (18):5701–5707, 1974.

[5] M. Lisal, W.R. Smith, and J. Kolafa. *J. Phys. Chem. B*, 109 (26):12956–12965, 2005.

[6] F. Moucka, M. Lisal, J. Skvor, J. Jirsak, I. Nezbeda, and W.R. Smith. *J. Phys. Chem. B*, 115 (24):7849–7861, 2011.

[7] F. Moucka, M. Lisal, and W.R. Smith. *J. Phys. Chem. B*, 116 (18):5468–5478, 2012.

[8] F. Moucka, I. Nezbeda, and W.R. Smith. *J. Chem. Phys.*, 139 (12):124505, 2013.

[9] F. Moucka, I. Nezbeda, and W.R. Smith. *J. Chem. Theory Comput.*, 11 (4):1756–1764, 2015.

[10] Z. Mester and A.Z. Panagiotopoulos. *J. Chem. Phys.*, 142 (4):044507, 2015.

[11] S. Deublein, J. Vrabec, and H. Hasse. *J. Chem. Phys.*, 136 (8):084501, 2012.

[12] S. Reiser, S. Deublein, J. Vrabec, and H. Hasse. *J. Chem. Phys.*, 140 (4):044504, 2014.

[13] H.J.C Berendsen, J.R. Grigera, and T.P. Straatsma. *J. Phys. Chem.*, 91 (24):6269–6271, 1987.

[14] S. Reiser, M. Horsch, and H. Hasse. *J. Chem. Eng. Data*, 59 (11):3434–3448, 2014.

[15] S. Reiser, M. Horsch, and H. Hasse. *J. Chem Eng. Data*, 60 (6):1614–1628, 2015.

[16] S. Reiser, M. Horsch, and H. Hasse. *Fluid Phase Equilib.*, 408:141–150, 2016.

[17] J.G. Powles, S. Murad, and P.V. Ravi. *Chem. Phys. Lett.*, 188 (1-2):21–24, 1992.

[18] S. Murad and J.G. Powles. *J. Chem. Phys.*, 99 (9):7271–7272, 1993.

[19] S. Murad, J.G. Powles, and B. Holtz. *Mol. Phys.*, 86 (6):1473–1483, 1995.

[20] F. Paritosh and S. Murad. *AIChE J.*, 42 (10):2984–2986, 1996.

[21] Y. Luo and B. Roux. *J. Phys. Chem. Lett.*, 1 (1):183–189, 2010.

[22] C.W. Glass, S. Reiser, G. Rutkai, S. Deublein, A. Koester, G. Guevara-Carrion, A. Wafai, M. Horsch, M. Bernreuther, T. Windmann, H. Hasse, and J. Vrabec. *Comput. Phys. Commun.*, 185 (12):3302–3306, 2014.

[23] J. Vrabec and H. Hasse. *Mol. Phys.*, 100 (21):3375–3383, 2002.

[24] C.G. Gray and K.E. Gubbins. Clarendon Press, Oxford, 1984.

[25] H.A. Lorentz. *Ann. Phys.*, 248:127–136, 1881.

[26] D. Berthelot. *Compt. Rend. Ac. Sc.*, 126:1703–1706, 1857–1858, 1898.

[27] J. Vrabec, Y. Huang, and H. Hasse. *Fluid Phase Equilib.*, 279 (2):120–135, 2009.

[28] J. Vrabec, J. Stoll, and H. Hasse. *J. Phys. Chem. B*, 105 (48):12126–12133, 2001.

[29] I. Joung and T.E. Cheatham, III. *J. Phys. Chem. B*, 112 (30):9020–9041, 2008.

[30] G. Guevara-Carrion, J. Vrabec, and H. Hasse. *J. Chem. Phys.*, 134 (7):(074508), 2011.

[31] H. Flyvbjerg and H.G. Petersen. *J. Chem. Phys.*, 91 (1):461–466, 1989.

[32] P.P. Ewald. *Ann. Phys.*, 64 (3):253–287, 1921.

[33] J.G. Kirkwood and F.P. Buff. *J. Chem. Phys.*, 17 (3):338–343, 1949.

[34] B. Widom. *J. Chem. Phys.*, 39 (11):2808–2812, 1963.

[35] W.J. Hamer and Y.C. Wu. *J. Phys. Chem. Ref. Data*, 1 (4):1047-1100, 1972.

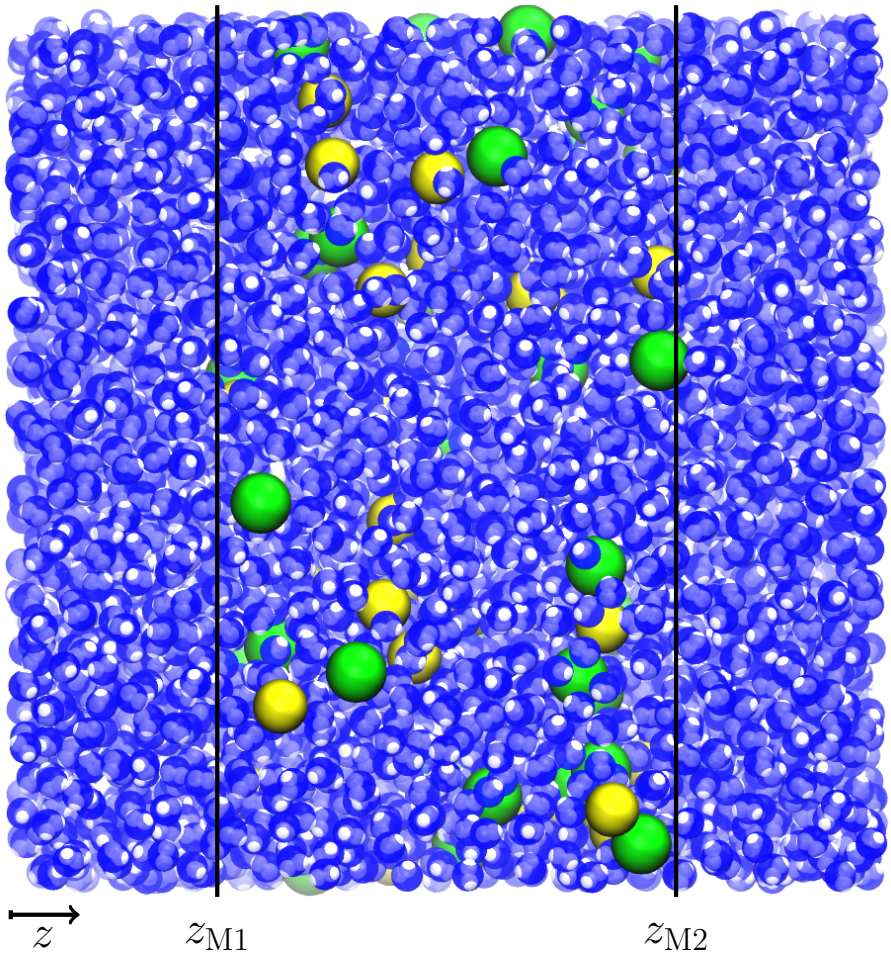

Figure 1: Snapshot from an OPAS simulation of an aqueous sodium chloride solution. The vertical lines indicate the positions of the two semipermeable membranes. Na^+ cations and Cl^- anions are shown as yellow and green spheres, respectively. Only the inner compartment of the simulation box is accessible to the ions. The oxygen atom of water is shown in blue, the hydrogen atoms of water are shown in white, and the size of the water molecules has been reduced for better visualization.

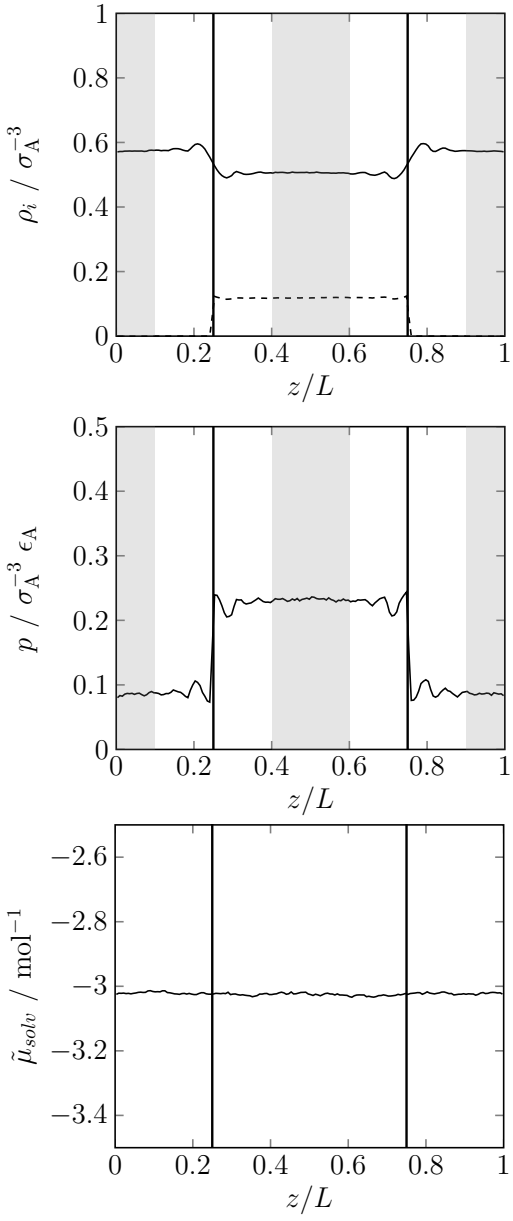

Figure 2: Partial density, pressure, and chemical potential profiles from OPAS simulation of a binary LJ mixture. Top: profiles of the reduced partial density for the solvent (component A, solid line) and the solute (component B, dashed line). Middle: profile of the reduced pressure. Bottom: profile of the reduced residual chemical potential of the solvent. All profiles are plotted versus the reduced coordinate normal to the membrane. The vertical lines indicate the positions of the two semipermeable membranes. The gray areas represent the inner and outer sampling volumes for the evaluation of the profiles. The box length is $L \approx 65.9$ Å.

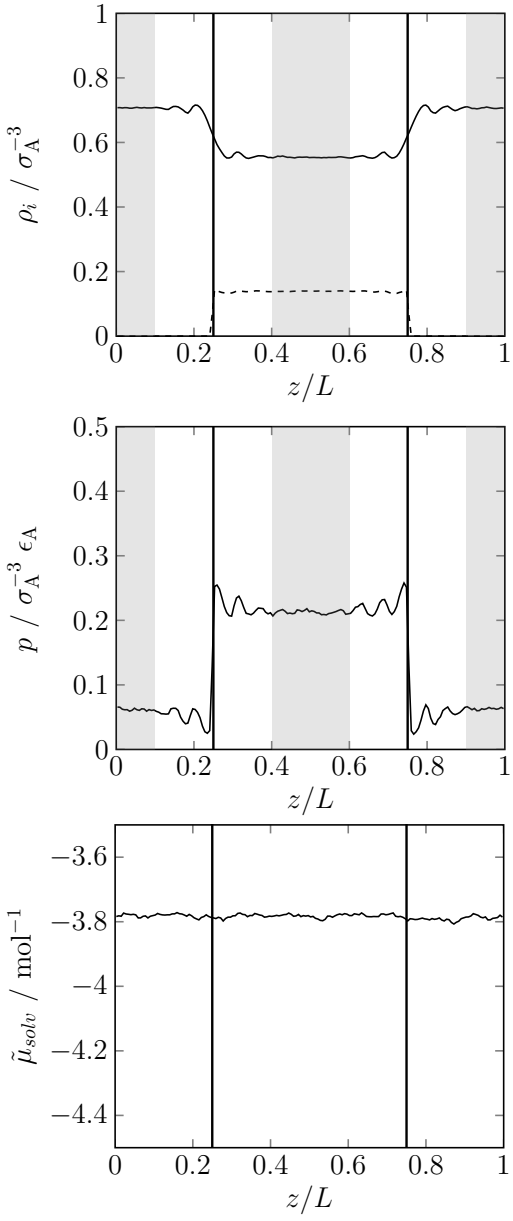

Figure 3: Partial density, pressure, and chemical potential profiles from OPAS simulation of an unlike LJ mixture. Top: profiles of the reduced partial density for the solvent (component A, solid line) and the solute (component B, dashed line). Middle: profile of the reduced pressure. Bottom: profile of the reduced residual chemical potential of the solvent. All profiles are plotted versus the reduced coordinate normal to the membrane. The vertical lines indicate the positions of the two semipermeable membranes. The gray areas represent the inner and outer sampling volumes for the evaluation of the profiles. The box length is $L \approx 62.6$ Å.

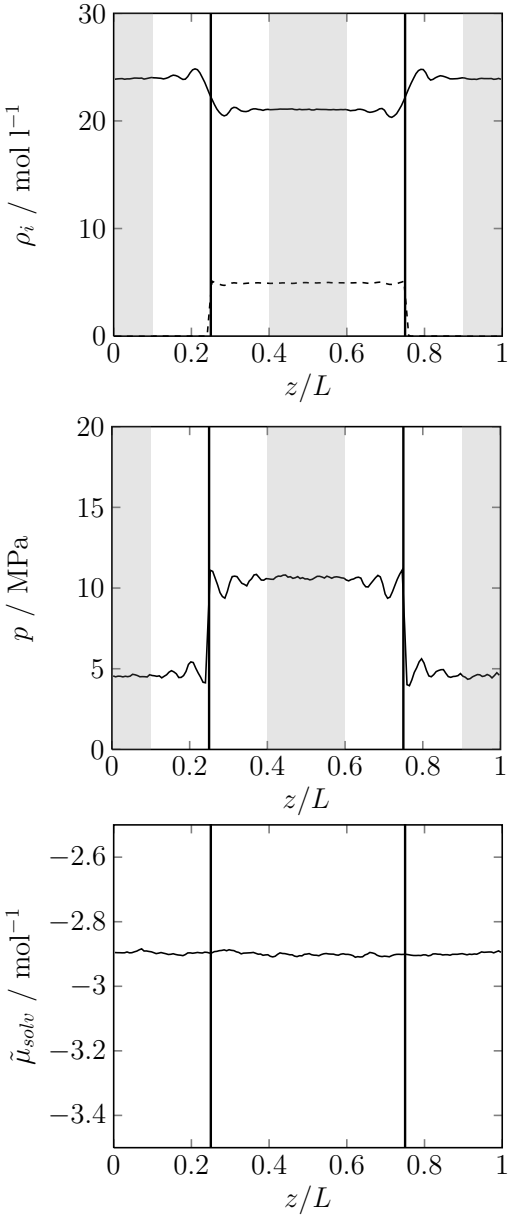

Figure 4: Partial density, pressure, and chemical potential profiles from OPAS simulation of mixture of argon and O_2. Top: profiles of the reduced partial density for the solvent argon (solid line) and the solute O_2 (dashed line). Middle: profile of the reduced pressure. Bottom: profile of the reduced residual chemical potential of the solvent. All profiles are plotted versus the reduced coordinate normal to the membrane. The vertical lines indicate the positions of the two semipermeable membranes. The gray areas represent the inner and outer sampling volumes for the evaluation of the profiles. The box length is $L \approx 63.5$ Å.

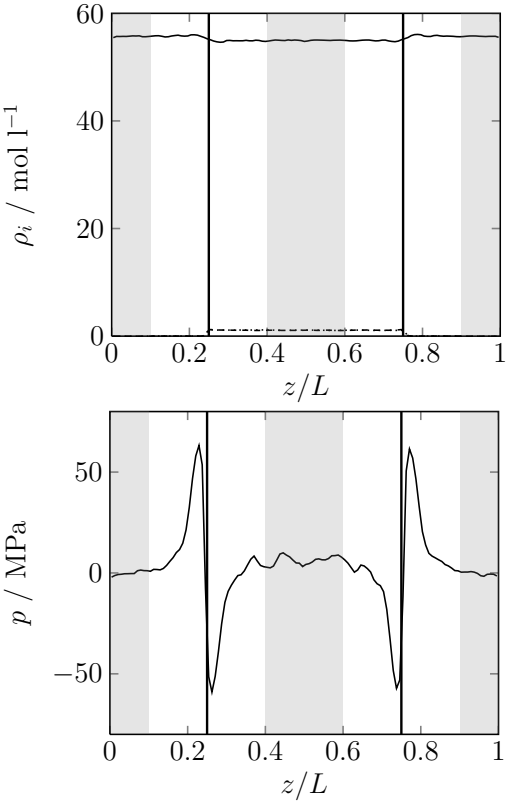

Figure 5: Partial density and pressure profiles from OPAS simulation of an aqueous NaCl solution using the SPC/E + JC [29] model combination. Top: profiles of the partial density for the solvent water (solid line) and the ions Na^+ (dashed line) and Cl^- (dotted line). These two lines for the density of the ions are undiscernable. The salt molality evaluated from the density profile is $m \approx 1.14$ mol kg^{-1}. Bottom: profile of the pressure. Both profiles are plotted versus the reduced coordinate normal to the membrane. The vertical lines indicate the positions of the two semipermeable membranes. The gray areas represent the inner and outer sampling volumes for the evaluation of the profiles. The box length is $L \approx 49.0$ Å.

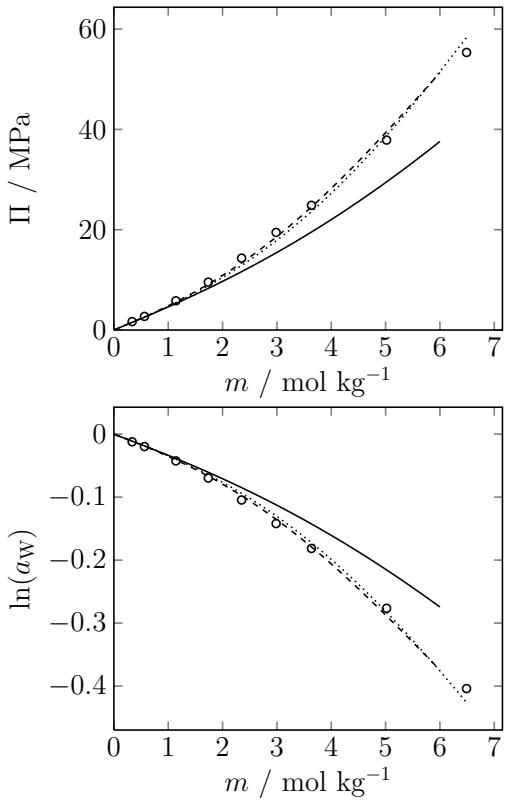

Figure 6: Osmotic pressures (top) and water activity (bottom) over the salt molality for aqueous NaCl solutions using the SPC/E + JC [29] model combination. Present simulation results are shown as open circles, the statistical uncertainties are within symbol size. Correlations fitted to simulation results obtained by Mester and Panagiotopoulos [10] (dashed line) and by Moučka et al. [9] (dotted line) using the same molecular models as well as the correlation to experimental data by Hamer and Wu [35] (solid line) are also shown for comparison.

Test case	Molecular models	State point	osmotic pressure Δp	osmotic pressure Π
Binary LJ mixture	LJ $\sigma_B/\sigma_A = 1.0$ and $\epsilon_B/\epsilon_A = 1.0$	$T^* = 1.2$, $\rho^* = 0.6$, $N_A = 3600$, $N_B = 400$	0.146(3) $\epsilon_A \sigma_A^{-3}$	0.153(1) $\epsilon_A \sigma_A^{-3}$
Unlike LJ mixture	LJ $\sigma_B/\sigma_A = 1.0$ and $\epsilon_B/\epsilon_A = 0.66$	$T^* = 1.0$, $\rho^* = 0.7$, $N_A = 3600$, $N_B = 400$	0.150(3) $\epsilon_A \sigma_A^{-3}$	0.148(1) $\epsilon_A \sigma_A^{-3}$
Ar + O_2 mixture	Ar and O_2 models by Vrabec et al. [28], $\xi_{Ar,O2}$=0.988 adjusted by Vrabec et al. [27]	$T = 140$ K, $\rho = 26$ mol l^{-1}, $N_{Ar} = 3600$, $N_{O2} = 400$	6.1(1) MPa	6.33(3) MPa
Aqueous NaCl solution	SPC/E [13] for water, JC [29] for Na^+ and Cl^-	$T = 298.15$ K, $p_{out} = 1$ bar, $N_W = 3920$, $N_{Na^+} = N_{Cl^-} = 40$	7(1) MPa	6.0(1) MPa

Table 1: Overview of test cases for the novel OPAS simulation method. The osmotic pressure Δp is obtained from the pressure profile, and Π is obtained by sampling the membrane force. Statistical uncertainties are given in parentheses.

m_{NaCl} / mol kg^{-1}	Π / MPa	$\ln(a_{\mathrm{W}})$
0.3358(2)	1.67(6)	−0.0122(4)
0.5628(4)	2.72(7)	−0.0198(5)
1.141(1)	5.8(1)	−0.0425(8)
1.738(2)	9.6(1)	−0.070(1)
2.350(3)	14.3(2)	−0.105(1)
2.985(4)	19.5(2)	−0.142(2)
3.636(4)	24.9(2)	−0.182(2)
5.018(7)	37.9(3)	−0.277(2)
6.49(1)	55.3(4)	−0.404(3)

Table 2: Osmotic pressure and activity of water at $T = 298.15$ K and varying salinity obtained by OPAS simulation for aqueous NaCl solutions using the SPCE + JC [29] model combination. Statistical uncertainties are given in parentheses.